PAPER

Check for updates

Sr$_3$YLi(PO$_4$)$_3$F:Eu^{2+},Ln^{3+}: colorless-magenta photochromism and coloration degree regulation through Ln^{3+} co-doping

Yang Lv, Yahong Jin,* Chuanlong Wang, Li Chen, Guifang Ju (iD) and Yihua Hu (iD) *

Herein, novel photochromic materials, Sr$_3$YLi(PO$_4$)$_3$F:Eu^{2+},Ln^{3+}, have been prepared by a conventional high-temperature solid-state reaction. Eu^{2+} singly doped Sr$_3$YLi(PO$_4$)$_3$F showed reversible colorless-magenta photochromism when alternately irradiated by UV and visible light (or thermal treatment). Thus, Sr$_3$YLi(PO$_4$)$_3$F:Eu^{2+} might be a potential candidate in various fields such as in imaging, sensors, photo-switches, and erasable optical storage media. The optimal Eu^{2+} doping concentration is experimentally determined to be about 0.5 mol%. The coloring and bleaching processes are attributed to electron trapping accompanied by the generation of F-centers and detrapping by different traps, respectively. Thus, these processes open a window for us to design a simple way to regulate and control the photochromic performance just by adjusting the doping concentration of Eu^{2+} ions or co-doping Ln^{3+} ions. On the basis of thermoluminescence, a schematic of a photochromic mechanism has also been proposed.

1. Introduction

The photochromic (PC) phenomenon was discovered more than one hundred years ago. Armistead and Stooky, two materials scientists at Corning studios in the United States, found the reversible photochromic properties of silver halide (AgX) glasses in the 1960s, which was the first time that a PC material was made for successful commercial application. The photochromic phenomenon refers to the reversible conversion between two forms or states accompanying significant changes in the absorption spectra induced in at least one direction by a certain wavelength of incident electromagnetic radiation.[1–5]

The PC materials have attracted increasing interests in scientific research not only due to color variation but also due to additional spontaneous variation such as in fluorescence, magnetic properties, oxidation/reduction potential, dielectric constant, electron conductivity, and refractive index.[6–9] These variations make them potentially applicable in various fields such as in erasable optical memory media, sensors, photo-optical switches, rewritable copy papers, and optical fibers and communications.[10–15] However, most of the reported PC materials are organic materials and inherit some natural drawbacks such as low fatigue resistance, environmentally harmful synthesis processes, and low thermal and chemical stability, which will restrict their commercial applications. In contrast, the inorganic PC materials have some better

characteristics, such as easily controllable macroscopic shape molding and high thermal and chemical stability, as compared to the organic counterparts. However, the research on inorganic PC materials is mostly concentrated on silver halides, alkali halides, alkaline earth halides, titanates, complex minerals, and transition metal oxide thin films such as WO$_3$, TiO$_2$, MoO$_3$, Nb$_2$O$_5$, and V$_2$O$_5$, which are usually in the form of thin films or single crystals, displaying poor PC reversibility and slow response rate. Relatively, inorganic PC materials as powders are more useful than in the form of thin films or single crystals because their surface color is suitable for reflective readout and possesses large area displays in ambient light.[16] Therefore, the development of new inorganic PC materials in powder form is still the critical challenge in practical applications.

In recent years, a series of inorganic PC materials in powder form has been reported such as Sr$_2$SnO$_4$:Eu^{3+}, Zn$_2$GeO$_4$:Eu^{2+}, BaMgSiO$_4$:Eu^{2+}, Ba$_5$(PO$_4$)$_3$Cl:Eu^{2+}, Sr$_3$YNa(PO$_4$)$_3$F:Eu^{2+}, Sr$_3$-GdLi(PO$_4$)$_3$F:Eu^{2+}, Sr$_3$GdNa(PO$_4$)$_3$F:Eu^{2+},Ln^{3+}, CaAl$_2$O$_4$:-Eu^{2+},Nd^{3+}, and Mg$_4$Ga$_8$Ge$_2$O$_{20}$:Cr^{3+}.[17–25] Based on the abovementioned materials, doping of europium ion into a proper host may be a good way to obtain novel PC materials, and many of these matrices are apatite-type structure. Ca$_{10}$(PO$_4$)$_6$F$_2$ is the first known apatite-type structure, which was discovered and named by Náray-Szábo. The apatite-type structure compounds are usually expressed as A$_{10}$(XO$_4$)$_6$Z$_2$, where A is a cation (K$^+$, Na$^+$, Li$^+$, Ca^{2+}, Sr^{2+}, Ba^{2+}, La^{3+}, Y^{3+}, Gd^{3+}, *etc.*), X is a cation (P^{5+}, Si^{4+}, Ge^{4+}, *etc.*), and Z is an anion (F$^-$, Cl$^-$, *etc.*).[26,27] Inspired by the abovementioned PC materials with excellent reversible photochromic performance and thermal and

School of Physics and Optoelectronic Engineering, Guangdong University of Technology, WaiHuan Xi Road, No. 100, Guangzhou 510006, China. E-mail: yhjin@gdut.edu.cn; huyh@gdut.edu.cn; Fax: +86 20 39322265; Tel: +86 20 39322262

chemical stability, we synthesized and studied the phosphors $Ba_5(PO_4)_3Cl:Eu^{2+}$, $Sr_3YNa(PO_4)_3F:Eu^{2+}$, $Sr_3GdLi(PO_4)_3F:Eu^{2+}$, and $Sr_3GdNa(PO_4)_3F:Eu^{2+},Ln^{3+}$ possessing photochromism with the abovementioned structure.[20–23]

As we can see, the phosphor of Eu^{2+}-doped $Sr_3YLi(PO_4)_3F$ (SYLP) has not been reported in literature. In this study, a fluorapatite-type photochromic material, SYLP:Eu^{2+}, is reported and its photochromism properties have been investigated further. Under excitation by UV light, the reflection spectrum of the SYLP:Eu^{2+} phosphor displays an intense and broad absorption ranging from 500 nm to 680 nm and reaches the extremum at 553 nm, and the surface of the phosphor changes from white to magenta. Moreover, when treated alternately by UV light irradiation and visible light or heating, SYLP:Eu^{2+} shows reversible color change with high fatigue resistance. Interestingly, color change adjustment can be achieved by Ln^{3+} co-doping. Thus, we can design and control the coloration degree by choosing different Ln^{3+} ions as co-dopants. Based on the thermoluminescence (TL) spectra, a more in-depth understanding of the photochromic mechanism, comprising the generation of a color center, the motion of electrons, and the theory of regulating the coloring degree, was realized. Finally, a schematic of the PC mechanism is also presented.

2. Experiment and characterization

2.1 Synthesis

A series of Eu^{2+} single-doped and Eu^{2+}-Ln^{3+} co-doped SYLP phosphors has been prepared through a high-temperature solid-state reaction. The starting materials are $SrCO_3$ (A.R.), SrF_2 (A.R.), Li_2CO_3 (A.R.), $(NH_4)_2HPO_4$ (A.R.), Y_2O_3 (99.99%), Eu_2O_3 (99.99%), and Ln_2O_3 (99.99%). The required raw materials according to the stoichiometry with 20% excess of SrF_2 were mixed and ground fully in an agate mortar. After being mixed thoroughly, the mixtures were moved to alumina crucibles. The mixtures were pre-sintered at 600 °C for 2 h. After being ground again, the mixtures were sintered at 1000 °C for 3 h under a reducing atmosphere ($N_2 : H_2 = 90\% : 10\%$), and the products were reground to a fine powder for the following measurements.

2.2 Characterization

The phases of all the obtained samples were identified by powder X-ray diffraction (XRD) analysis using a XD-2 powder diffractometer with Cu Kα irradiation ($\lambda = 1.5406$ Å) operating at 36 kV and 20 mA. Photoluminescence (PL) and photoluminescence excitation (PLE) spectra were obtained via a FLS-980 fluorescence spectrophotometer (Edinburgh Instruments) equipped with a Xe lamp (450W, Osram). UV-vis diffuse reflectance spectra were characterized by a UV-visible spectrophotometer (Evolution 220) with $BaSO_4$ as a reference. High-temperature diffuse reflectance spectra were obtained using the same UV-visible spectrophotometer equipped with a home-made heating device. Thermoluminescence (TL) curves were obtained from 30 to 450 °C by a thermoluminescence meter (SL08-L) at a heating rate of 5 °C s^{-1}. The electron paramagnetic

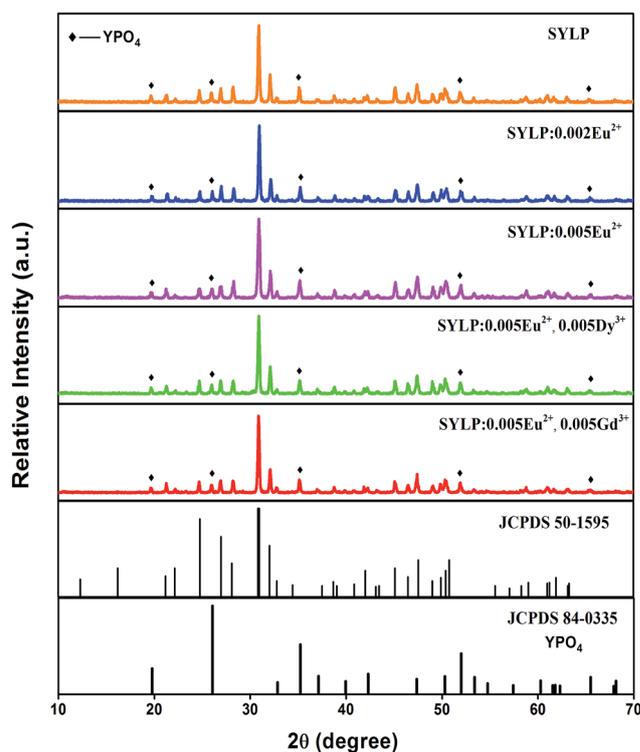**Fig. 1** XRD patterns of typical samples together with JCPDS standard data for $Sr_3(La,Ce)Na(PO_4)_3(F,OH)$ (No. 50-1595) and YPO_4 (No. 84-0335).

resonance (EPR) spectra were obtained using a JES-FA200 ESR spectrometer at a frequency of 9.198 GHz and at low temperature (90 K) in vacuum.

3. Results and discussion

3.1 Phase identification

To verify the phases of all obtained samples, XRD was used. Fig. 1 demonstrates the representative XRD patterns of the obtained phosphors together with the reference standard XRD data of $Sr_3(La,Ce)Na(PO_4)_3(F,OH)$ (Joint Committee on Powder Diffraction Standards (JCPDS) 50-1595). The patterns of the obtained samples cannot be indexed to any compounds that have been published in JCPDS. However, most diffraction peaks of the as-prepared samples can be indexed to the standard data JCPDS 50-1595 $Sr_3(La,Ce)Na(PO_4)_3(F,OH)$ except for a little impurity, which is possibly attributed to YPO_4, and the reference data of YPO_4 are listed in Fig. 1. The results reflect that the SYLP fluorophosphates are isostructural to the apatite-type $Sr_3LaNa(PO_4)_3F$ compounds, and Y^{3+} and Li^+ are doped to substitute La^{3+} and Na^+, respectively, due to the same valence and similar ionic radius.[28] When Eu^{2+} and Ln^{3+} are doped into the SYLP host lattice, there is no significant change in the XRD patterns. Based on the effective ionic radii and charge balance ($r_{Sr^{2+},CN=6} = 1.18$ Å, $r_{Eu^{2+},CN=6} = 1.17$ Å, $r_{Y^{3+},CN=6} = 0.90$ Å, $r_{Li^+,CN=6} = 0.76$ Å, $r_{Nd^{3+},CN=6} = 0.98$ Å, $r_{Gd^{3+},CN=6} = 0.94$ Å, $r_{Ce^{3+},CN=6} = 1.01$ Å, $r_{Dy^{3+},CN=6} = 0.91$ Å), we suggest that Eu^{2+} and Ln^{3+} ions take priority of replacing Sr^{2+} and Y^{3+}, respectively.
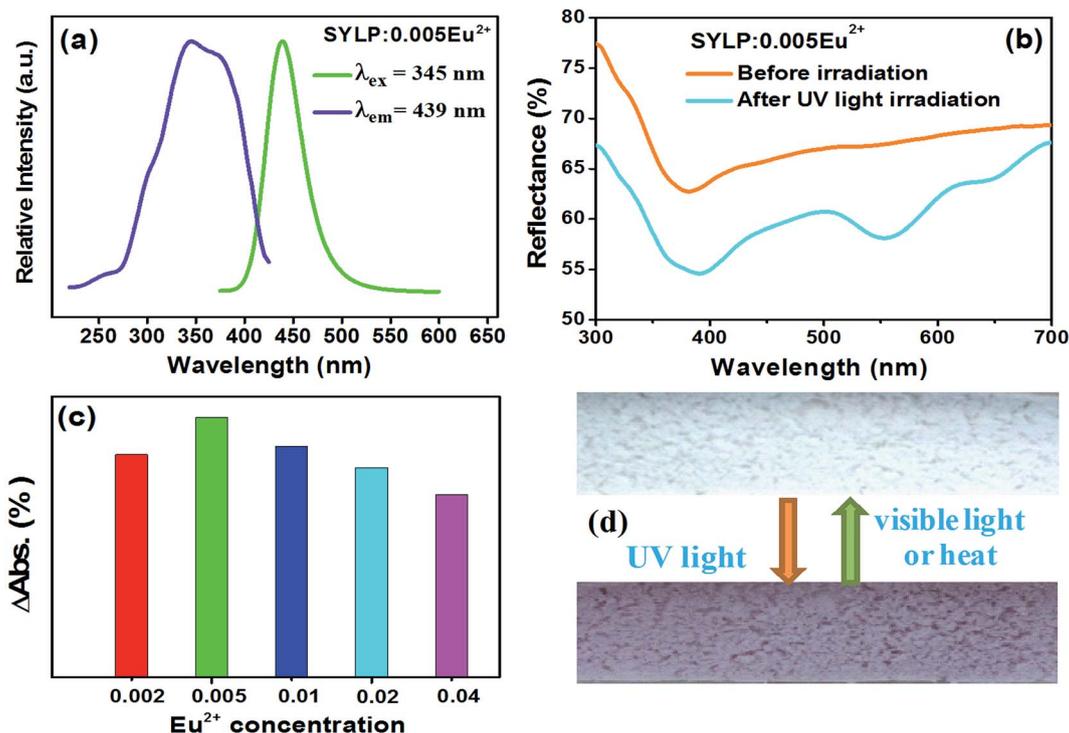
Fig. 2 (a) The PLE and PL spectra of the SYLP:0.005Eu^{2+} sample. (b) The reflectance spectrum of SYLP:0.005Eu^{2+} without and with UV light irradiation. (c) The ΔAbs of SYLP:xEu^{2+} (x = 0.002–0.04) after UV light irradiation. (d) The image of the sample before and after irradiation by UV light.

3.2 Photoluminescence and photochromism properties of SYLP:Eu^{2+}

Fig. 2(a) depicts photoluminescence (PL) and photoluminescence excitation (PLE) spectra of the SYLP:0.005Eu^{2+} phosphor. Monitored at 439 nm, the spectrum shows a broad excitation band ranging from 230 to 420 nm, with the maximal value at 310 nm, which is caused by the 4f^7 → 4f^{6}5d^1 transition of Eu^{2+} ions. Under the excitation by 310 nm, the PL spectrum displays a wide emission band ranging from 400 to 550 nm centering at 439 nm, which is ascribed to the 4f^{6}5d^1 → 4f^7 transition of Eu^{2+} ion.

The diffuse reflectance spectra of SYLP:0.005Eu^{2+} before and after 254 nm light irradiation for 3 min are shown in Fig. 2(b). Apparently, a wide absorption can be discovered in the region from 500 to 680 nm, attaining the maximum at 553 nm after 254 nm light irradiation. The surface of the sample changes from colorless to magenta, and the image of the sample surface under UV and visible light irradiation is displayed in Fig. 2(c). Notably, the doping concentration of Eu^{2+} in the SYLP host plays a critical role in adjusting the coloring degree. The ΔAbs is defined as R_b–R_a, where R_b is the reflectivity before irradiation by UV light and R_a is the reflectivity after irradiation by UV light. Thus, the relationship between ΔAbs at 553 nm and doping concentration of Eu^{2+} is shown in Fig. 2(d). It can be clearly seen that the ΔAbs first increases, attains the maximum at x = 0.005, and then continues to decrease. With the greater value of the ΔAbs, the surface color change becomes more intense; this

proves that the doping concentration of Eu^{2+} is a critical factor in the determination of coloration degree. Based on the results, it can be known that with the increase of Eu^{2+} content, the photochromic effect of SYLP:Eu^{2+} increases at first, approaching the maximum, and then decreases; thus, the best doping concentration of Eu^{2+} ion has been identified as 0.005.

Moreover, the TL curves of SYLP:xEu^{2+} (x = 0.002–0.04) samples are shown in Fig. 3(a). It can be seen that they have similar shape. The TL intensity increases at first, reaching the maximum when x = 0.005, and then continuously declines; this indicates that the TL intensity is largely dependent on the contents of Eu^{2+}. The TL intensity of SYLP:xEu^{2+} and their ΔAbs at 553 nm in Fig. 2(c) show the similar change tendency; this proves that PC performance is closely related to traps. The Gauss fitting of SYLP:0.005Eu^{2+} is displayed in Fig. 3(b). It shows two different peaks centering at about 92 and 200 °C, and the intensity at lower temperature is higher than that at high temperature. Based on Fig. 3(b), it means that the electrons in the shallow traps are almost emptied when heated to 150 °C. To prove that photochromism is related to deep traps or shallow traps, we attempted to empty the shallow traps by heating. Fig. 4(a) indicates the TL curves of SYLP:0.005Eu^{2+} with and without heat treatment at 150 °C. When the sample is heated to 150 °C before the TL measurement, it can be clearly seen that the TL intensity significantly decreases at lower temperatures and is not observed basically, and the decay rate at higher temperatures is evidently slower than that at low temperatures. Moreover, Fig. 4(b) shows the reflection spectra of the sample
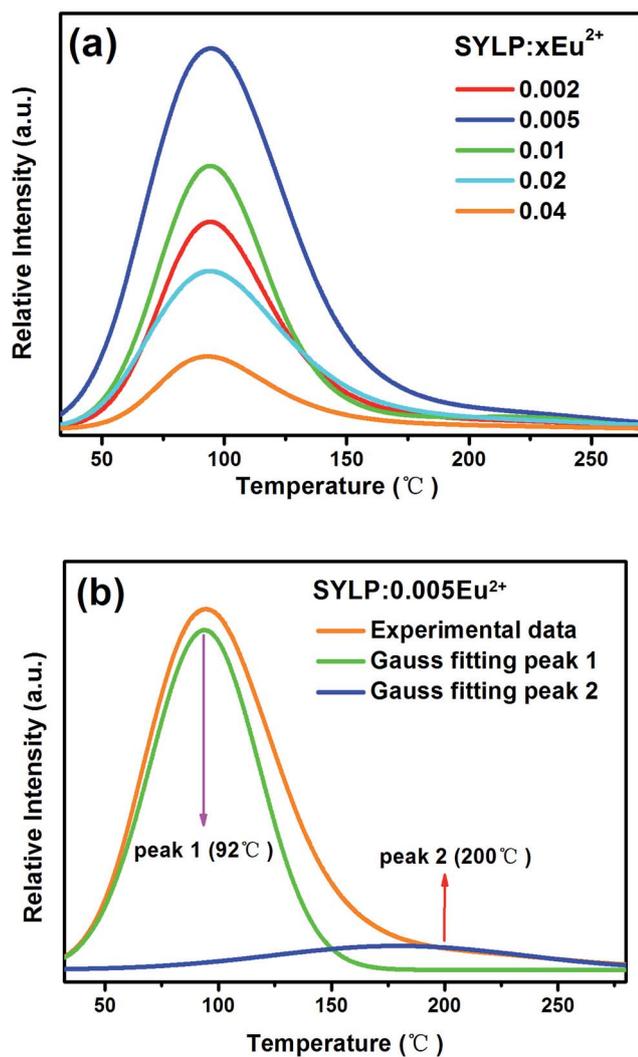
Fig. 3 (a) The TL curves of SYLP:xEu^{2+} ($x = 0.002-0.04$). (b) The Gauss fitting of SYLP:0.005Eu^{2+}.

Fig. 4 (a) TL curves of SYLP:0.005Eu^{2+} with and without heat treatment at 150 °C. (b) The reflection spectra of the sample with and without UV light irradiation and the reflection spectrum of the coloring sample heated at 150 °C.

with and without UV light irradiation and the reflection spectrum of the coloring sample after being heated to 150 °C. As shown in Fig. 4(b), it still has a partial absorption at 500–680 nm after being heated to 150 °C; this means that the colored sample maintains a certain coloring degree and is not completely bleached; this demonstrates that the deep traps are the crucial factor of photochromism. The trap depth can be calculated by the following equation.[29,30]

$$E = T_{\mathrm{m}}/500 \qquad (1)$$

where T_{m} is the temperature at the TL peak; the depth of traps can be calculated as 0.73 and 0.95 eV. Normally, although the depth of the trap is about equal to 0.7 eV, it is quite suitable for charge carriers escaping and producing persistent luminescence at room temperature.[31] However, the electrons in deeper traps are difficult to be released and will survive longer.[32] Therefore, we can infer that the coloring state will not vanish
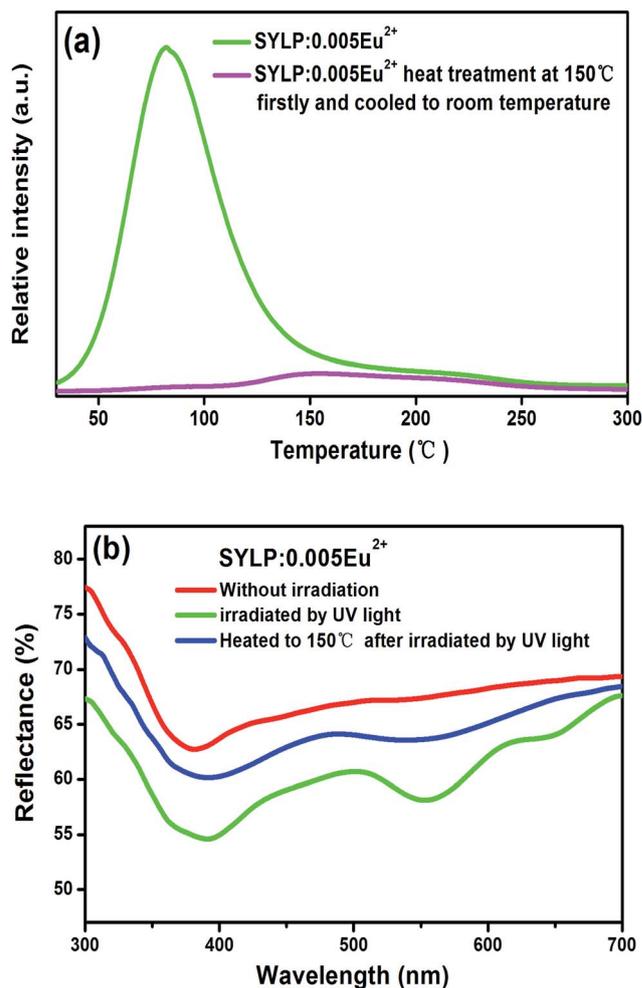
immediately, nor will it disappear in a short time without external stimulation.

Reversibility is an important feature of PC materials. Therefore, the reflectance change of the SYLP:0.005Eu^{2+} sample under the alternating UV and visible light irradiation for several cycles is shown in Fig. 5(a). The sample surface varied between colorless and magenta. It shows a high reversibility in the processes of coloring and bleaching. The results illustrate that the SYLP:Eu^{2+} phosphors have good repetition in recording and erasing information, inferring that the SYLP:Eu^{2+} phosphor may be a candidate that can be applied in photoswitches and erasable optical memory devices. PC performance is associated with traps; this suggests that heat treatment may have a significant effect on colored samples. Based on this, the reflectance change of the SYLP:0.005Eu^{2+} sample upon alternate UV light irradiation and heat treatment for several loops is shown in Fig. 5(b). The reflectivity of the SYLP:0.005Eu^{2+} sample at 553 nm returns to the initial level when the temperature is
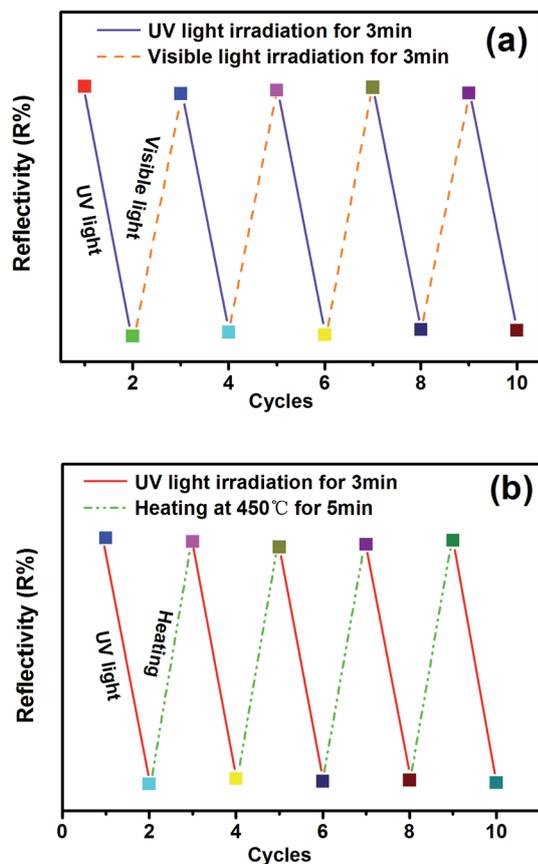
Fig. 5 (a) The reflectance change of SGLPF:0.005Eu^{2+} at 553 nm irradiated by alternating UV and visible light. (b) The reflectance change of SGLPF:0.005Eu^{2+} at 553 nm by alternating UV light illumination and heat treatment at 400 °C.

increased to 450 °C and is maintained for 5 min. Evidently, heating to high temperature can cause the accelerated bleaching of the colored samples, and the bleached sample can be colored again under UV light irradiation.

3.3 Coloring degree regulation of SYLP:Eu^{2+} through Ln^{3+} doping

The long afterglow properties of some materials can be regulated by doping rare earth ions.[33,34] Similarly, we consider that it is possible to achieve the coloration degree regulation through Ln^{3+} ion co-doping in the obtained SYLP:Eu^{2+} PC materials. To demonstrate this conjecture, a series of SYLP:Eu^{2+},Ln^{3+} materials has been synthesized, and the results indicate that it shows different effects on PC property *via* different Ln^{3+} ion co-doping.

The ΔAbs at 553 nm corresponding to different Ln^{3+} coping is shown in Fig. 6. Eu^{2+} single-doped SYLP is used as a blank for comparison. Obviously, the ΔAbs values at 553 nm are strengthened or weakened by co-doping different Ln^{3+} ions; this infers that the coloration is enhanced or reduced. The ΔAbs can be strengthened by the incorporation of Ho^{3+} ions; this indicates that the coloring degree is enhanced. By comparison, when Nd^{3+}, Sm^{3+} or Dy^{3+} ions are co-doped into SYLP:Eu^{2+}, the ΔAbs values are slightly lowered. The ΔAbs values of other Ln^{3+}
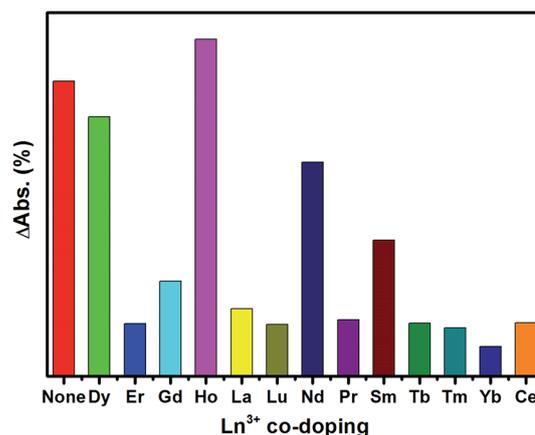

Fig. 6 The ΔAbs of samples at 553 nm by co-doping different Ln^{3+} ions.

ion co-doped samples display significant decrease; this indicates that the coloration degree is largely weakened. According to the abovementioned results, we suppose that doping of different Ln^{3+} ions into SYLP:Eu^{2+} photochromic materials will have different impacts on the traps; this will lead to the enhancement or reduction of coloration degree. Accordingly, Ln^{3+} ions can be divided into three groups: (I) Ho^{3+}, where the co-doping ions can cause the ΔAbs to increase obviously; (II) Nd^{3+}, Sm^{3+}, and Dy^{3+}, where they can lead to a slight decrease of ΔAbs; and (III) Gd^{3+}, Lu^{3+}, Pr^{3+}, La^{3+}, Tm^{3+}, Er^{3+}, Ce^{3+}, Tb^{3+}, and Yb^{3+}, where the co-doping of these rare earth ions will lead to significant reduction of the ΔAbs.

To explain the traps that are controlled and modulated by co-doping of Ln^{3+} ions, TL spectra of the obtained SYLP:0.005Eu^{2+},0.005Ln^{3+} samples are characterized with the SYLP:0.005Eu^{2+} sample as a reference. The TL spectra of three groups are displayed in Fig. 7(a)–(c). As shown in Fig. 7(a), it can be clearly seen that the predominating peak moves from low temperature to high temperature and locates at around 193 °C, and the TL intensity increases, evidently corresponding to coloration deepening that matches with the increase of ΔAbs in Fig. 6. Fig. 7(b) indicates that the predominated peak also shifts to high temperatures, but the TL intensity significantly decreases; this is in agreement with the reduction of ΔAbs in Fig. 6; this demonstrates that the PC property is weakened slightly. As shown in Fig. 7(c), the third class of ions not only leads to the predominated peak that has slightly shifted to lower temperatures, but also exhibits strong decrease in TL intensity, coinciding with the poor PC property and significant decrease of ΔAbs in Fig. 6.

3.4 The EPR measurement of SYLP:0.005Eu^{2+}

EPR is an effective way to research the coordination environment of Eu^{2+} ions.[34] Fig. 8 depicts EPR measurements of the SYLP:0.005Eu^{2+} sample with and without UV light illumination for 5 min together with the colored sample under the re-irradiation by visible light for 10 min that were performed at 90 K in vacuum. The obtained EPR signals are relevant to the
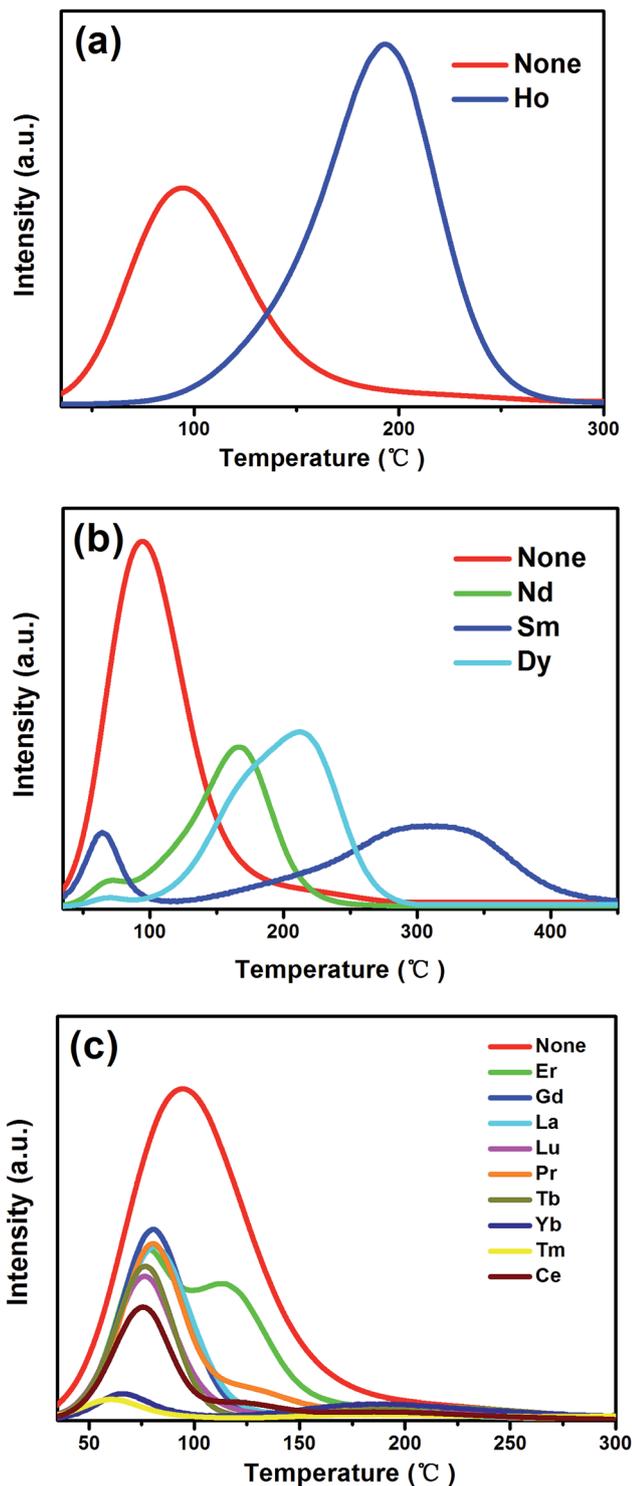
Fig. 7 (a) TL spectra of the SYLP:0.005Eu²⁺ sample and SYLP:0.005Eu²⁺,0.005Ho³⁺. (b) TL spectra of SYLP:0.005Eu²⁺,0.005Ln³⁺ sample (Ln = Nd, Dy, and Sm). (c) TL spectra of SYLP:0.005Eu²⁺,0.005Ln³⁺ sample Ln = Gd, Lu, Pr, La, Tm, Er, Ce, Tb, and Yb.

overlap of clustered Eu^{2+} ions and paramagnetic singly ionized oxygen vacancy $(V_o^{\cdot})$.[21,35–37] The EPR spectra of two sharp signals are displayed in Fig. 8(a) and (b), representing the resonance

signals characteristic of Eu^{2+} ions.[38] Upon UV light irradiation, the intensities of signals, as shown in Fig. 8(a) and (b), are reduced and have a recovery trend after illumination by visible light; this infers that Eu^{2+} ions are converted to Eu^{3+} ions *via* photo-oxidation, and the F-like color centers are formed under illumination by UV light, and then, the captured electrons go back to Eu^{3+} by visible light illumination. As shown in Fig. 8(c), under the irradiation by UV light, a significant increase takes place in the intensity of the EPR signal; this indicates that numerous $V_o^{\cdot}$ are produced. The EPR signal intensity shows a recovery trend after visible light irradiation; this demonstrates the decrease of $V_o^{\cdot}$ and the conversion of Eu^{3+} ions to Eu^{2+} ions. In addition, the captured electrons will be rapidly released from $V_o^{\cdot}$ traps under external stimuli, such as photostimulation and heat treatment, that would reduce Eu^{3+} ions to Eu^{2+} ions.

3.5 The PC mechanism of SYLP:Eu²⁺

Based on the abovementioned results and discussion, the PC and coloration degree regulation mechanism are presented in Fig. 9. Under irradiation by longer UV light, the electrons in the ground level of Eu^{2+} can only be pumped to the lower 5d level and then transferred to the lowest 5d level through nonradiative relaxation. Finally, the electrons move back to the ground level, accompanied by blue emission. Upon excitation by shorter UV light, the electrons in the Eu^{2+} ground level can be excited to the high 5d levels, which are located above or near the bottom of the conduction band (CB). On the one hand, a majority of excited electrons immediately move back to the ground level, and a blue emission will be observed, which originates from Eu^{2+}. On the other hand, the residual excited electrons might be transferred into the CB with the aid of thermal energy although with a small possibility under ambient condition. The electrons will be trapped by the oxygen vacancies that are located near the photogenerated Eu^{3+} cations.[22] Eu^{2+} ions and Eu^{3+} ions are stabilized in the oxide. Moreover, Eu^{2+} ions can be oxidized by UV light; therefore, Eu^{2+} ions and Eu^{3+} ions can survive together in the SYLP host. Furthermore, the F-like color centers are formed by the captured electrons, and the sample surface changes from white to magenta. At room temperature, the captured electrons easily escape from shallow traps, but their escape is quite hard from deep traps. As a result, the colored sample presents a fast fading process and a slow fading process in the dark at room temperature.[39] Stimulated by external factors, for instance, long wavelength irradiation and heat treatment, the trapped electrons in the traps are immediately released into the CB that will be caused by a faster bleaching process. By co-doping Ln^{3+} ions into the SYLP host, the distribution of traps can be adjusted. (I) Ln^{3+} = Ho^{3+}, it not only greatly increases the depth of a deep trap, but also enhances the integral trap density largely, such that the coloring degree enhancement is achieved. (II) Ln^{3+} = Dy^{3+}, Nd^{3+}, and Sm^{3+}, these ions greatly enhance the deep trap depths, but significantly reduce the integral trap density; this leads to the reduction of coloration degree. (III) Ln^{3+} = Er^{3+}, Gd^{3+}, La^{3+}, Lu^{3+}, Pr^{3+}, Tb^{3+}, Tm^{3+}, Yb^{3+}, and Ce^{3+}; in these cases, the depth of the deep trap is significantly reduced, and the integral trap density is markedly decreased; this results in the reduction of the coloration degree.
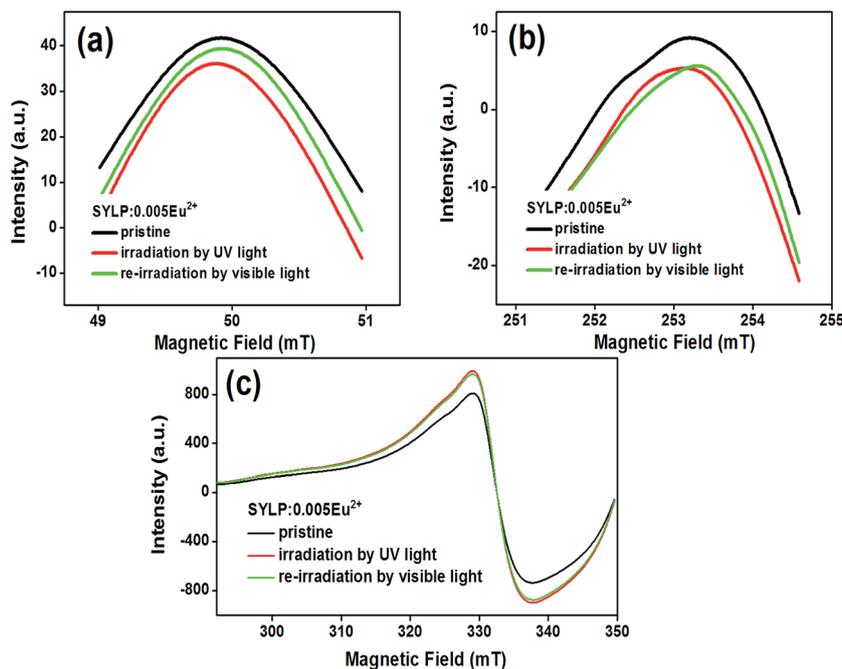
Fig. 8 The EPR spectra of SYLP:0.005Eu^{2+} before and after UV light illumination together with re-irradiation by visible light.
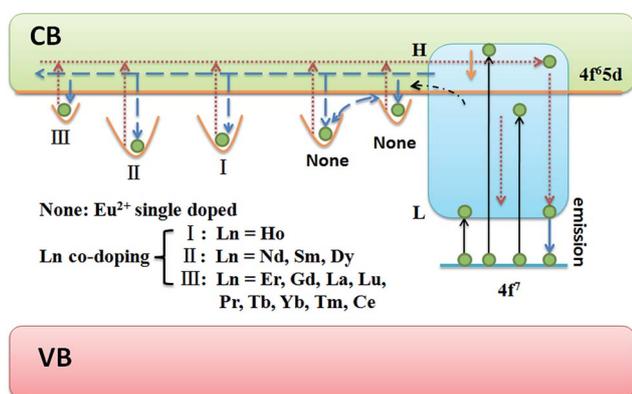
Fig. 9 The model for interpretation of the PC mechanism.

According to the obtained results, the $Sr_3YLi(PO_4)_3F:Eu^{2+},Ln^{3+}$ PC materials might have potential applications for erasable optical storage medium and sensors.

Conflicts of interest

There are no conflicts to declare.

Acknowledgements

4.   Conclusion

To summarize, a series of novel photochromic $Sr_3YLi(PO_4)_3$-$F:Eu^{2+},Ln^{3+}$ powder materials has been obtained by a traditional high-temperature solid-state reaction. It is interesting that the surface of the sample changes between white and magenta under alternate irradiation of UV and visible light or heat treatment. Thus, the good PC reversibility and thermal stability of the as-prepared SYLP:Eu^{2+} sample are proven. The reversible PC property is attributed to the conversions between Eu^{2+} and Eu^{3+} ions. The optimum doping concentration of Eu^{2+} ion is determined to be about 0.5 mol%. To further investigate the PC phenomenon, we have achieved the adjustment of coloration degree by Ln^{3+} ion co-doping, which is inspired by trap modulation. A model is proposed, and the explanation for the generation and regulation of PC phenomenon is summarized.

References

1 E. Hadjoudis and I. M. Mavridis, *Chem. Soc. Rev.*, 2004, **33**, 579–588.
2 Y. Ohko, T. Tatsuma, T. Fujii, K. Naoi, C. Niwa, Y. Kubota and A. Fujishima, *Nat. Mater.*, 2003, **2**, 29–31.
3 R. Exelby and R. Grinter, *Chem. Rev.*, 1965, **65**, 247–260.
4 M. M. Russew and S. Hecht, *Adv. Mater.*, 2010, **22**, 3348–3360.
5 M. Irie, *Chem. Rev.*, 2000, **100**, 1685–1716.
6 Q. Zhang, X. Zheng, H. Sun, W. Li, X. Wang, X. Hao and S. An, *ACS Appl. Mater. Interfaces*, 2016, **8**, 4789–4794.
7 J. Ren, X. Xu, W. Shen, G. Chen and S. Baccaro, *Sol. Energy Mater. Sol. Cells*, 2014, **143**, 635–639.
8 J. Zhang, Q. Zou and H. Tian, *Adv. Mater.*, 2013, **25**, 378–399.
9 M. Taguchi, T. Nakagawa, T. Nakashima and T. Kawai, *J. Mater. Chem.*, 2011, **21**, 17425–17432.

10 J. Ren, T. Wagner, J. Orava, M. Frumar and B. Frumarova, *Appl. Phys. Lett.*, 2008, **92**, 011114.

11 A. J. Cohen and H. L. Smith, *Science*, 1962, **137**, 981.

12 J. Yao, K. Hashimoto and A. Fujishima, *Nature*, 1992, **355**, 624–626.

13 P. Zacharias, M. C. Gather, A. Köhnen, N. Rehmann and K. Meerholz, *Angew. Chem., Int. Ed.*, 2009, **48**, 4038–4041.

14 G. Poirier, M. Nalin, L. Cescato, Y. Messaddeq and S. J. Ribeiro, *J. Chem. Phys.*, 2006, **125**, 161101.

15 A. Bianco, S. Perissinotto, M. Garbugli, G. Lanzani and C. Bertarelli, *Laser Photonics Rev.*, 2011, **5**, 711–736.

16 R. Duncan, B. Faughnan and W. Phillips, *Appl. Opt.*, 1970, **9**, 2236–2243.

17 S. Kamimura, H. Yamada and C.-N. Xu, *Appl. Phys. Lett.*, 2013, **102**, 031110.

18 Y. H. Jin, Y. H. Hu, Y. R. Fu, Z. F. Mu and G. F. Ju, *Mater. Lett.*, 2014, **134**, 187–189.

19 M. Akiyama, *Appl. Phys. Lett.*, 2010, **97**, 181905.

20 G. Ju, Y. Hu, L. Chen and X. Wang, *ECS Solid State Lett.*, 2012, **1**, R1–R3.

21 Y. H. Jin, Y. H. Hu, Y. R. Fu, L. Chen, G. F. Ju and Z. F. Mu, *J. Mater. Chem. C*, 2015, **3**, 9435–9443.

22 Y. Lv, Y. H. Jin, C. L. Wang, G. F. Ju, F. H. Xue and Y. H. Hu, *J. Lumin.*, 2017, **186**, 238–242.

23 Y. H. Jin, Y. Lv, C. L. Wang, G. F. Ju, H. Y. Wu and Y. H. Hu, *Sens. Actuators, B*, 2017, **245**, 256–262.

24 S. Kamimura, H. Yamada and C. N. Xu, *Appl. Phys. Lett.*, 2013, **102**, 031110.

25 Y. H. Jin, Y. H. Hu, L. F. Yuan, L. Chen, H. Y. Wu, G. F. Ju, H. Duan and Z. F. Mu, *J. Mater. Chem. C*, 2016, **4**, 6614–6625.

26 Y. Zhang, G. G. Li, D. L. Geng, M. M. Shang, C. Peng and J. Lin, *Inorg. Chem.*, 2012, **51**, 11655–11664.

27 H. K. Liu, Y. Luo, Z. Y. Mao, L. B. Liao and Z. G. Xia, *J. Mater. Chem. C*, 2014, **2**, 1619–1627.

28 R. D. Shannon, *Acta Crystallogr., Sect. A: Cryst. Phys., Diffr., Theor. Gen. Crystallogr.*, 1976, **32**, 751–767.

29 P. F. Li, M. Y. Peng, L. Wondraczek, Y. Q. Zhao and B. Viana, *J. Mater. Chem. C*, 2015, **3**, 3406–3415.

30 R. Chen, *J. Appl. Phys.*, 1969, **40**, 570–585.

31 R. Sakai, T. Katsumata, S. Komuro and T. Morikawa, *J. Lumin.*, 1999, **85**, 149–154.

32 V. D. E. Koen, A. J. J. Bos, D. Poelman and P. F. Smet, *Phys. Rev. B: Condens. Matter Mater. Phys.*, 2013, **20**, 196.

33 Y. Li, B. H. Li, C. C. Ni, S. X. Yuan, J. Wang, Q. Tang and Q. Su, *Chem.–Asian J.*, 2014, **9**, 494–499.

34 W. Zeng, Y. Wang, S. Han, W. Chen and G. Li, *Opt. Mater.*, 2014, **36**, 1819–1821.

35 D. K. Patel, A. Sengupta, B. Vishwanadh, V. Sudarsan, R. K. Vatsa, R. Kadam and S. K. Kulshreshtha, *Eur. J. Inorg. Chem.*, 2012, **2012**, 1609–1619.

36 L.-C. Ju, X. Xu, L.-Y. Hao, Y. Lin and M.-H. Lee, *J. Mater. Chem. C*, 2015, **3**, 1567–1575.

37 J. B. Priebe, M. Karnahl, H. Junge, M. Beller, D. Hollmann and A. Brückner, *Angew. Chem., Int. Ed.*, 2013, **52**, 11420–11424.

38 V. Singh, R. P. S. Chakradhar, J. L. Rao and H.-Y. Kwak, *J. Lumin.*, 2011, **131**, 247–252.

39 H. Guo, Y. Wang, W. Chen, W. Zeng, S. Han, G. Li and Y. Li, *J. Mater. Chem. C*, 2015, **3**, 11212–11218.